

Environmental Science and Pollution Research manuscript No.
(will be inserted by the editor)

1 **Taking full advantage of modelling to better assess**

2 **environmental risk due to xenobiotics**

3 **Sandrine Charles^{*1} · Aude Ratier^{*1} ·**

4 **Virgile Baudrot¹ · Gauthier Multari ·**

5 **Aurélie Siberchicot¹ · Dan Wu ·**

6 **Christelle Lopes¹**

7 Received: date / Accepted: date

This work was performed using the computing facilities of the CC LBBE/PRABI. This work benefited from the French GDR “Aquatic Ecotoxicology” framework which aims at fostering stimulating scientific discussions and collaborations for more integrative approaches. This work is part of the ANR project APPROve (ANR-18-CE34-0013) for an integrated approach to propose proteomics for biomonitoring: accumulation, fate and multi-markers (<https://anr.fr/Projet-ANR-18-CE34-0013>).

*

These two authors equally contributed.

1

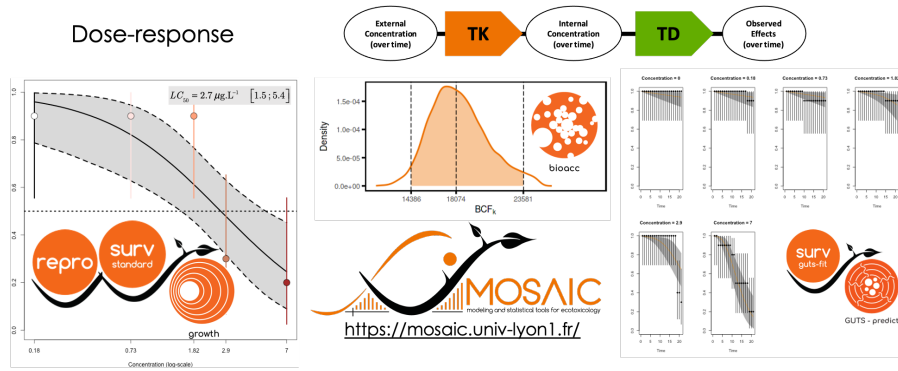
Université de Lyon, Université Lyon 1, CNRS UMR5558, Laboratoire de Biométrie et Biologie Evolutive, 69100 Villeurbanne, France. E-mail: sandrine.charles@univ-lyon1.fr

8 **Abstract** In the European Union, more than 100,000 man-made chemical
9 substances are awaiting an environmental risk assessment (ERA). Simultane-
10 ously, ERA of chemicals has now entered a new era. Indeed, recent recommen-
11 dations from regulatory bodies underline a crucial need for the use of mechanis-
12 tic effect models, allowing assessments that are not only ecologically relevant,
13 but also more integrative, consistent and efficient. At the individual level,
14 toxicokinetic-toxicodynamic (TKTD) models are particularly encouraged for
15 the regulatory assessment of pesticide-related risks on aquatic organisms. In
16 this paper, we first propose a brief review of classical dose-response models
17 to put into light the on-line MOSAIC tool offering all necessary services in a
18 turnkey web platform whatever the type of data to analyze. Then, we focus on
19 the necessity to account for the time-dimension of the exposure by illustrating
20 how MOSAIC can support a robust calculation of bioaccumulation factors. At
21 last, we show how MOSAIC can be of valuable help to fully complete the EFSA
22 workflow regarding the use of TKTD models, especially with GUTS models,
23 providing a user-friendly interface for calibrating, validating and predicting
24 survival over time under any time-variable exposure scenario of interest. Our
25 conclusion proposes a few lines of thought for an even easier use of modelling
26 in ERA.

27

28 **Keywords** dose-response models · bioaccumulation factors · toxicokinetic-
29 toxicodynamic model · uncertainty · accessibility

30 **Graphical art**



31 1 Introduction

32 Effects of contaminants may occur at all levels of biological organization, from
33 molecular to ecosystem-level responses (Clements, 2000). From one level to
34 the next the answers to exposure may strongly differ, from DNA damage
35 metabolism disorders to loss of biodiversity or changes in food web structures.
36 Hence, an effective translation of information through increasing organization
37 levels (e.g., from individual to population) will provide more ecologically rel-
38 evant endpoints as stated by the adverse outcome pathway concept (Ankley
39 et al., 2010), together with increased temporal and spatial scales of the un-
40 derlying processes. At the opposite, going down at inferior levels of biological
41 organisation is crucial to finely decipher the underlying mechanisms and their
42 specificity (Preuss et al., 2009). From the molecular to the ecosystem scales,
43 each individual, population and community levels may appear to be the best
44 compromise between ecological relevance and understanding of mechanisms.
45 This explains why the vast majority of mathematical models focus on a specific
46 biological scale, while few allow for extrapolation between these levels.

47 Whatever the level of biological organization, there are challenges for which
48 mathematical models are or will be crucial. At the community level, we can
49 mainly distinguish two categories of models. Some models consider a commu-
50 nity as a set of species chosen to be representative of a given ecosystem without
51 modelling the between-species interactions; this is the case with species sen-
52 sitivity distributions (SSD), based on fitting probability distributions. They
53 are used in ERA for extrapolating among species and across levels of bio-

54 logical organization, but they are overly simplistic and likely to lead to both
55 over-estimates and under-estimates of risk (Forbes & Calow, 2002; Forbes &
56 Galic, 2016). Other models, based on ordinary (ODE) or partial (PDE) differ-
57 ential equations, will aim to describe the community functioning accounting
58 for all types of ecological interactions as done for example by AQUATOX, the
59 simulation model for aquatic systems from US EPA (Park et al., 2008).

60 At the population level, the key issue is to include individual effect mod-
61 els to refine the prediction of population dynamics. Indeed, effects of chem-
62 ical substances do not depend only on exposure and toxicity, but also on
63 factors such as life history characteristics and population structure. Popula-
64 tion models are also helpful to identify critical demographic traits regarding
65 given species-compound combinations. As reviewed in Schmolke et al. (2010),
66 population models are mainly based on ODE/PDE, projection matrices or
67 individual-based approaches. Although a broad range of these ecological mod-
68 els is available in the scientific literature, they are still rarely used in support
69 of regulatory ERA (Schmolke et al., 2010), probably due to their inherent
70 complexity and a lack of easy tools in order to run them, except home-made
71 computer codes rather designed for specialists.

72 In this paper, we focus on the individual level, where modelling has been
73 prominent for a long time already with dose-response (DR) models providing
74 toxicity values (namely, standard lethal LC_x or effective EC_x concentrations)
75 allowing to identify critical life history traits for given species-compound com-
76 binations (Ritz, 2010). Nevertheless, scientific knowledge still remain poor re-

77 guarding the physiological modes of action of compounds and how they vary
78 across species and compounds (Ashauer & Jager, 2018). Additionally, authori-
79 ties today recognize the need to account for the time-dependency of the effects
80 to better assess risk under complex exposure situations (e.g., environmentally
81 realistic concentrations, various exposure routes, biotransformation processes,
82 mixture effects). To this end, the toxicokinetics (TK) and the toxicodynamics
83 (TD) of the effects require to be modelled. The TK part relates the exposure
84 concentration to the internal concentration within organisms, considering var-
85 ious processes such as accumulation, depuration, metabolization and excretion
86 (ADME). TK models are typically used to calculate bioaccumulation factors
87 from data collected in standard bioaccumulation tests (OECD, 2012) and new
88 perspectives are offered by a recent modelling approach (Ratier et al., 2019) as-
89 sociated with a ready-to-use tool (Ratier et al., 2020). The TD part makes the
90 link between damages suffered by organisms due to internal bioaccumulated
91 concentrations with observable effects on life history traits such as an increased
92 mortality or a reduced growth. Combined TKTD models are recommended by
93 EFSA to refine Tier-2 risk assessment, especially for plant protection products
94 acting on aquatic organisms when exposed to time-variable exposure profiles
95 (European Commission, 2013; Ockleford et al., 2018; Brock et al., 2020). In
96 particular, the EFSA already considers ready-to-use for ERA the TKTD mod-
97 els dedicated to the prediction of survival over time, and the EFSA encourages
98 more research for the other types of TKTD models, namely those based on
99 the Dynamic Energy Budget (DEB) theory for growth and reproduction of ec-

100 totherm species and those for macrophytes. The reason why General Unified
101 Threshold models for Survival (GUTS models) are already operable in sup-
102 port of the daily work of regulators is the availability of a general framework
103 that unify all of survival models, as well as easily accessible, user-friendly and
104 transparent turnkey tools, allowing to run them with only several user actions.
105 Tools for GUTS models are also known to provide reproducible results, with-
106 out the need for the users to invest in underlying mathematical and statistical
107 aspects (Jager & Ashauer, 2018).

108 Among available modelling tools dedicated to ecotoxicity, the MOSAIC
109 platform proposes a suite of services within an all-in-one web site. MOSAIC is
110 an acronym for MOdelling and StAtistical tools for ecotoxICology, that can be
111 accessed through any Internet browser at <https://mosaic.univ-lyon1.fr/>
112 (MOSAIC, 2013). Available since 2013, MOSAIC first proposed a service
113 for SSD analyses via $MOSAIC_{SSD}$ (Kon Kam King et al., 2014; MOSAIC-
114 *ssd*, 2013). In 2014, two additional services, namely $MOSAIC_{surv}$ (MOSAIC-
115 *surv*, 2014) and $MOSAIC_{repro}$ (MOSAICrepro, 2014) (details in Charles et al.
116 (2018)), were offered to estimate classical toxicity values from standard sur-
117 vival and reproduction data, respectively, providing LC_x and EC_x . In 2018, a
118 new facility was integrated allowing to calibrate, validate and predict survival
119 from GUTS models under time-variable exposure profiles: $MOSAIC_{GUTS-fit}$
120 (MOSAICguts-fit, 2018) in combination with $MOSAIC_{GUTS-predict}$ (MOSAICguts-
121 *predict*, 2018; Baudrot et al., 2018b). At last, in 2020, two last services were
122 offered: (i) $MOSAIC_{growth}$ (MOSAICgrowth, 2020) delivering EC_x estimates

123 from standard continuous data (such as length, weight, growth rate,...), mak-
124 ing then available a full suite of services for standard analyses whatever the
125 type of data collected via standard toxicity tests (Charles et al., 2021); (ii)
126 MOSAIC_{bioacc} (MOSAICbioacc, 2020) fitting a variety of TK models account-
127 ing for several routes of exposure, several elimination processes and several
128 phase-I metabolites from one parent compound (Ratier et al., 2019), from
129 which bioaccumulation factors are automatically derived (Ratier et al., 2020).
130 All MOSAIC modules make available a collection of example data sets, allow-
131 ing new users to practice using the various features.

132 The purpose of this article is to present all the features of MOSAIC in or-
133 der to guide academics, manufacturers and regulators to benefit from advanced
134 and sound models in ERA in support of their daily work, meeting all expect-
135 tations in terms of regulatory requirements. The first section gives insights on
136 classical DR analyses, focusing on the last new-born service MOSAIC_{growth}.
137 The second section illustrates how to get bioaccumulation factors from TK
138 models, with a focus on the selection of different models to be compared, and
139 how to fulfil the EFSA workflow regarding the use of GUTS models for ERA
140 (Ockleford et al., 2018). The last section aims at convincing the reader of the
141 added-value of GUTS models for Tier-1 risk assessment when LC_x are re-
142 quired. Finally, the conclusion proposes concrete lines of thought to make the
143 use of modelling in environmental risk assessment even easier.

144 2 Classical dose-response modelling

145 2.1 Few words about modelling

146 When performing standard analyses of toxicity test data in MOSAIC, the
147 mean tendency of the relationship between the observed endpoints and the
148 tested concentrations is first described by a 3-parameters log-logistic model
149 written as follows:

$$f(C) = \frac{d}{1 + \left(\frac{C}{e}\right)^b} \quad (1)$$

150 where C stands for the tested concentration, parameter b is a shape pa-
151 rameter translating the intensity of the effect, d corresponds to the endpoint
152 value in control data (*i.e.*, in absence of contaminant) and e corresponds to
153 the EC_{50} , that is the C value leading to 50% of effect compared to the control
154 (*i.e.*, compared to parameter d): $f(e) = \frac{d}{2}$. Equation (1) also assumes that
155 $\lim_{C \rightarrow +\infty} f(C) = 0$.

156 Then, depending on the endpoints that are observed, the variability around
157 the mean tendency is described by an appropriately chosen probability dis-
158 tribution. Quantal (or binary) data (*e.g.*, survival data) are associated with
159 a binomial distribution. Count data (*e.g.*, reproduction data) are associated
160 with a Poisson distribution, possibly combined with a Gamma distribution
161 in case of over-dispersion. Quantitative continuous data, namely data with
162 a unit such as length or weight for example, are associated with a Normal

163 (Gaussian) distribution. For example, in case of quantitative continuous data,
164 the final model writes as follows:

$$y_{obs}(C) \sim \mathcal{N}(f(C), \sigma^2) \quad (2)$$

165 where $y_{obs}(C)$ stands for observations at concentration C , $f(C)$ for the
166 deterministic part (equation1) and σ for the standard deviation of the Normal
167 law \mathcal{N} .

168 Such a writing means that a total of four parameters must be estimated
169 from observed data: b , d , e and σ . Within MOSAIC, except in MOSAIC_{SSD},
170 all parameters are inferred under a Bayesian framework requiring to define
171 prior distributions on parameters. These are automatically provided by MO-
172 SAIC based on the experimental design associated with the data as uploaded
173 by the user. Prior distributions are then combined to the likelihood (whose
174 writing depends on the probability law chosen to describe the variability
175 within the data) to finally provide the joint posterior probability distribu-
176 tion informing on parameter estimates, their uncertainty and their correla-
177 tions. Both modelling and inference processes are run automatically in MO-
178 SAIC without any action from the user to get the final results, except a
179 single click. More information about modelling is available in Charles et al.
180 (2018); Baudrot et al. (2018a); Charles et al. (2021); Ratier et al. (2020). MO-
181 SAIC also provides detailed information via several links: a modelling tutorial
182 for MOSAIC_{surv} and MOSAIC_{repro} at [https://cran.r-project.org/web/](https://cran.r-project.org/web/packages/morse/vignettes/modelling.pdf)
183 [packages/morse/vignettes/modelling.pdf](https://cran.r-project.org/web/packages/morse/vignettes/modelling.pdf), for MOSAIC_{growth} at <http://>

184 lbbe-shiny.univ-lyon1.fr/mosaic-growth/vignette.pdf and for MOSAIC_{bioacc}
185 at [http://lbbe-shiny.univ-lyon1.fr/mosaic-bioacc/data/user_guide.](http://lbbe-shiny.univ-lyon1.fr/mosaic-bioacc/data/user_guide.pdf)
186 [pdf](#), respectively. The subsection below illustrates how to perform to a stan-
187 dard DR analysis from MOSAIC_{growth}. MOSAIC_{growth} has been developed in
188 R (R Core Team, 2021) within a Shiny environment (Chang et al., 2021)

189 2.2 MOSAIC_{growth}

190 Measuring growth of organisms (*e.g.*, length of shoots, dry weight of plants,
191 algal growth rate, size of daphnids) consists in collecting continuous quanti-
192 tative data to be fitted with a DR model. MOSAIC_{growth} provides all useful
193 outputs of the fitting process to check the relevance of the results, among
194 which estimates of the effective concentration for several $x\%$ of interest, typi-
195 cally a table of EC_x (or $x\%$ Effective Rates in the field of non-target terrestrial
196 plants). A total of 13 example data sets, concerning various species-compound
197 combinations, are provided for new users to practice.

198 MOSAIC_{growth} makes it possible to analyse one or several data sets si-
199 multaneously (Figure 1.A), by default at the last exposure time. Regarding
200 EC_x estimates, MOSAIC_{growth} output is the posterior probability distribu-
201 tion of the last EC_x requested by the user, as well as a summary table of all
202 EC_x estimates if several of them have been requested by the user (1.B). This
203 table includes not only the median and the 95% uncertainty interval of the
204 EC_x estimates, but also censored EC_x values determined by taking into ac-
205 count the uncertainty on the estimate relatively to the range of tested concen-

206 trations (see Charles et al. (2021) for details, or [http://lbbe-shiny.univ-](http://lbbe-shiny.univ-lyon1.fr/mosaic-growth/vignette.pdf)
207 [lyon1.fr/mosaic-growth/vignette.pdf](http://lbbe-shiny.univ-lyon1.fr/mosaic-growth/vignette.pdf)). These censored EC_x values can
208 further be used for SSD analyses with $MOSAIC_{SSD}$ (Kon Kam King et al.,
209 2014).

210 $MOSAIC_{growth}$ also provides a visualization of the DR fit at the chosen
211 exposure time (1.C). A table summarizes parameter estimates given as me-
212 dian values and their 95% uncertainty interval. In addition, goodness-of-fit
213 criteria are provided (1.D) associated with short explanations on what is ex-
214 pected, in order to guide the user in checking the relevance of its results. A
215 full tutorial is also available at [http://lbbe-shiny.univ-lyon1.fr/mosaic-](http://lbbe-shiny.univ-lyon1.fr/mosaic-growth/Tutorial.pdf)
216 [growth/Tutorial.pdf](http://lbbe-shiny.univ-lyon1.fr/mosaic-growth/Tutorial.pdf), especially the appendix where "no ideal" situations
217 are presented in support of this check. In order to ensure full transparency
218 and reproducibility of analyses, $MOSAIC_{growth}$ offers the possibility of down-
219 loading various types of document, including the entire R code (1.E).

220 Finally, $MOSAIC_{growth}$ offers a prediction tool to simulate a DR model
221 and predict the expected relationship between a range of concentrations that
222 the users may choose and what they can potentially achieve as effect at the
223 final time of their experiment (1.F). Such a tool can be particularly helpful in
224 designing future experiments for a given species-compound combination.

225 **3 Accounting for the time-dependency of the effects**

226 From a modelling point of view, the better way to account for the time-
227 dependency of the effects is the use of TKTD models relating the exposure



Fig. 1 Selected pieces from the $MOSAIC_{growth}$ web interface during DR analysis with the data set *plant07*: (A) upload of experimental data and visualization; (B) EC_x estimates for $x = 5, 10, 25, 50, 75$ and 90% obtained from the results of the DR model fit and graphical representation of the probability distribution of the EC_{90} ; (C) fitted model superimposed to the observed data: median curve (solid orange line) and its uncertainty (gray area delimited by orange dotted lines) with a summary of the estimated parameters; (D) example of two model fit criteria provided by the web interface (left: ‘Posterior Predictive Check’ (PPC); right: priors and posteriors); (E) result downloading; and (F) examples with the prediction tool for a series of concentrations (40, 80, 160, 320 and 640) (left: parameters not distributed; right: distributed parameters obtained from a previous DR analysis performed with $MOSAIC_{growth}$).

228 concentration to effects on individual life history traits via a more or less re-

229 fined description of the internal damages within organisms. TKTD models

230 allow to understand rather than to describe effects as built from underlying

231 mechanisms. TKTD models provide time-independent toxicity parameters (as

232 for example a no effect concentration), with outputs independent on both the

233 experimental design and the exposure duration. TKTD models also allow to

234 deal with time-varying exposure and to make predictions for untested situa-
235 tions. Above all, TKTD models allow to account for all collected data over
236 time, while standard DR analyses only focus on a given target time (usu-
237 ally, the last exposure time). Section 4 will show how this may be of crucial
238 importance for ERA.

239 All TKTD models can be presented according to a general scheme (Figure
240 2). Their specificities are related to the way both TK and TD parts are de-
241 fined. Regarding TK models, all are compartment models based on ordinary
242 differential equations, with one (the organism as a whole) or more compart-
243 ments depending on their refinement. When several compartments are involved
244 in TK models, different types are considered: either fictitious compartments
245 (TK compartment models) or each compartment corresponding to a specific
246 organ (physiologically-based (PB) TK models). Regarding the TD part, the
247 type of models depends on the described endpoints: effects on survival (lethal
248 effects) may be described by GUTS models, effects on plant growth (e.g., on
249 macrophyte growth rate) may be described by plant models, while effects on
250 growth and reproduction may simultaneously be described by toxicity mod-
251 els derived from the Dynamic Energy Budget (DEB) theory, that is DEBtox
252 models (Ockleford et al., 2018).

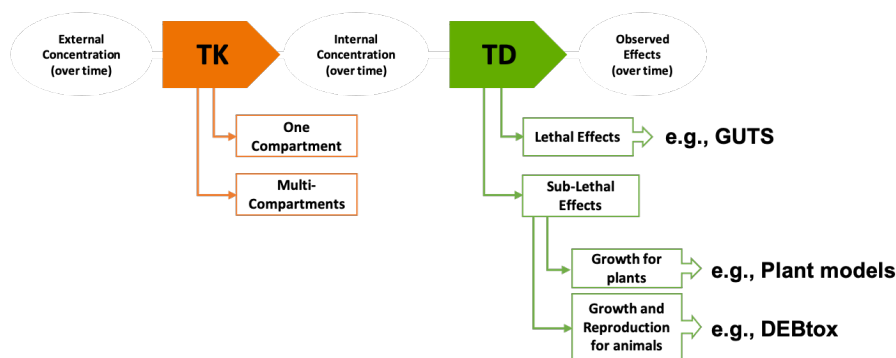


Fig. 2 A general scheme of toxicokinetic (TK) and toxicodynamic (TD) models; GUTS stands for the General Unified Threshold model of Survival, while DEBtox stands for toxicity models derived from the Dynamic Energy Budget (DEB) theory (from Ockleford et al. (2018)).

253 3.1 TK models

254 3.1.1 Few words about TK modelling

255 Chemicals are becoming potentially toxic if they bioaccumulate into the body
256 of organisms and after being transported to a target site where they will exert
257 effects. Chemicals may also undergo biotransformation into metabolites, which
258 may be more or less toxic themselves. And chemicals may be eliminated from
259 the body of organisms, for example by faeces or a phenomenon of dilution
260 by growth. All compartment TK models assume that chemicals are evenly
261 distributed within the compartment(s) what simplifies equations.

262 The most complete and complex TK models are PBTK models associating
263 compartments to organs or physiological fluids (*e.g.*, blood) and describing
264 in very details all chemical fluxes between compartments; they are mostly
265 available for aquatic species such as fish species and a number of chemical
266 classes including plant protection products, metals, persistent organic pollu-

267 tants, nano-particles (see Grech et al. (2017) for a review). The simplest TK
268 model has one compartment that corresponds to one organism, in which chem-
269 icals enter (at rate k_u) and from which chemicals are eliminated (at rate k_e).
270 This only-one compartment TK model will basically consider one exposure
271 route and one elimination process. In the regulatory ERA, such models are
272 fitted to data collected during bioaccumulation tests, which consists in an ac-
273 cumulation phase followed by a depuration phase. Estimates of parameters k_u
274 and k_e are then used to calculate bioaccumulation factors (OECD, 2012).

275 Nevertheless, even if the most complex TK models are not always required,
276 the very simple one reveals very limited when chemicals are present in several
277 media, so that organisms may be exposed via several routes, and/or when
278 several processes of elimination need to be accounted for, especially when a
279 parent compound may biotransform into metabolites. Such situations today
280 benefit from both a unified modelling framework (Ratier et al., 2019) and
281 a ready-to-use tool, $MOSAIC_{bioacc}$ (Ratier et al., 2020). The section below
282 illustrates the use of the last updated version of $MOSAIC_{bioacc}$.

283 *3.1.2 MOSAIC_{bioacc}*

284 $MOSAIC_{bioacc}$ is a newly offered service in MOSAIC since 2020 which has been
285 developed in R (R Core Team, 2021) within a Shiny environment (Chang
286 et al., 2021). It allows the estimation of bioaccumulation factors associated
287 with their uncertainty from the fit of a TK model, with only one compartment
288 corresponding to the whole organism but several exposure routes and several

289 elimination processes may be accounted for¹. The model is automatically built
290 according to the accumulation-depuration data uploaded by the user (Figure
291 3.A). By a single click, the user first obtains the posterior probability distri-
292 bution of the kinetic bioaccumulation factor (Figure 3.B), summarized with
293 its median and its 95% uncertainty interval (bounded by the 2.5% and 97.5%
294 percentiles of the posterior distribution, Figure 3.C). The uploaded data may
295 come from different types of experiments in which different routes of expo-
296 sure are considered (*e.g.*, surface water, pore water, sediment, food), as well as
297 different elimination processes (*e.g.*, excretion, biotransformation and growth
298 dilution). Fitting results are plotted (Figure 3.D) superimposed to the data
299 for the parent and its metabolites (if concerned). TK model parameters (*e.g.*,
300 k_u and k_e in the most simple situation) are also provided as medians and
301 95% uncertainty intervals (Figure 3.E). Then automatically come a number
302 of goodness-of-fit criteria to guide the users in checking the relevance of their
303 results (Figure 3.F). $MOSAIC_{bioacc}$ provides the same goodness-of-fit criteria
304 as $MOSAIC_{growth}$, also with a short description of the expected outputs and
305 cross-references to the tutorial illustrating and explaining what to do in non-
306 ideal situations. To ensure the reproducibility and the transparency of the
307 TK analyses, $MOSAIC_{bioacc}$ allows downloading all outputs under different
308 formats, as well as the entire R code used (Figure 3.G).

309 Several updates were recently implemented in $MOSAIC_{bioacc}$. First, it is
310 now possible to account for the lipid fraction within organisms in calcula-

¹ To access to the very last version of $MOSAIC_{bioacc}$ that is regularly updated and tested before to be deployed on the official server, please go to <https://scharles-univlyon1.shinyapps.io/mosaic-bioacc-gamma/>.

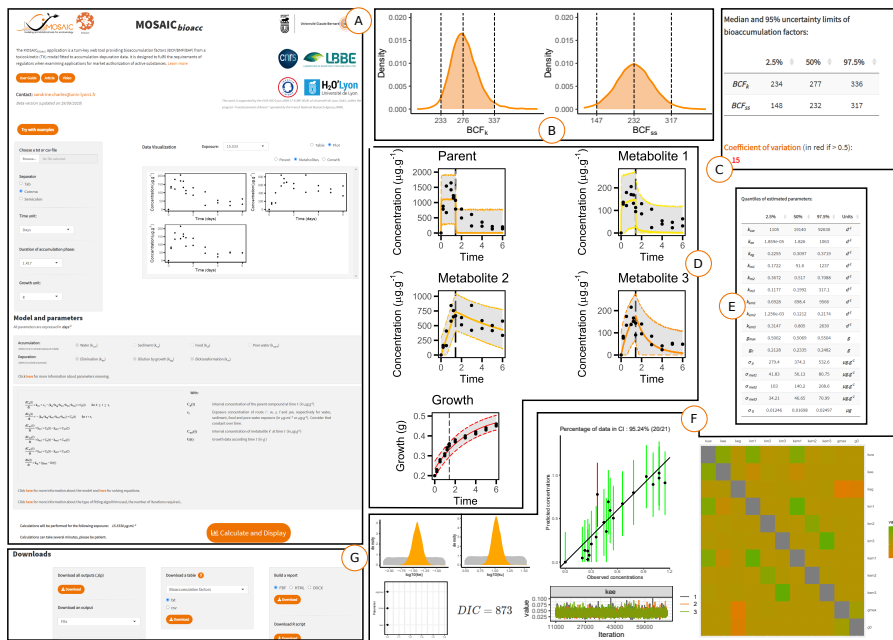


Fig. 3 Selected pieces from MOSAIC_{bioacc} when performing a TK analysis on two sample data sets: *Oncorhynchus_two* and *Male.Gammarus_seanine*: (A) upload of experimental data and simplified summary of the TK model and its parameters (automatically delivered); (B) graphical representation of bioaccumulation factors (here the kinetic BCF with example *Oncorhynchus_two*); (C) the corresponding statistical summary of the BCF distribution; (D) TK model fit (concentration in the body as a function of time): median curve (solid colored line) and its uncertainty (gray area delimited by colored dotted lines); (E) estimation of model parameters fitted to bioaccumulation data; (F) various model goodness-of-fit criteria; (G) result downloading the results.

311 tions; users just need to enter their measured value. Secondly, MOSAIC_{bioacc}

312 allows users to fit several nested TK models on a same data set. In practice,

313 users just need to choose the parameters they want to appear in sub-models.

314 According to the experimental conditions, several sub-models can indeed be

315 considered and compared depending on the hypotheses to test either on the

316 exposure routes or on the elimination processes. As illustrated in a case study

317 in supplementary information (see full report in SI), organisms may have been

318 exposed via several media (water and sediment in the case study in SI). By

319 default, MOSAIC_{bioacc} fits the full TK model. Then users can test different
320 TK sub-models, for example sub-models with only one exposure route (water
321 or sediment in the case study in SI), and compare them to the full model based
322 on both the Deviance Information Criteria (DIC) and the Watanabe–Akaike
323 information criterion (WAIC) delivered by MOSAIC_{bioacc}. Users can also test
324 different TK sub-models ignoring some of the elimination processes even if
325 they have been measured (*e.g.*, neglecting the dilution by growth). Hence, users
326 have now the possibility to choose the most appropriate TK model regarding
327 their data. Third, a collection of more than 80 data sets is made available to
328 support all features of MOSAIC_{bioacc}. More than 95% of these data sets are
329 published in the scientific literature. They encompass more than 25 species
330 (aquatic, terrestrial, insect), more than 66 chemical substances, different ex-
331 posure routes (water, sediment, soil, food) and several elimination processes
332 (biotransformation and growth dilution). This data collection is presented as
333 a table that summarises the main characteristics of the data (genus, category,
334 substance, accumulation duration, exposure routes, number of data and repli-
335 cates), as well as a direct link to the reference, and direct links to download
336 the raw data and the full report provided by MOSAIC_{bioacc}. In addition, the
337 table also gives the kinetic bioaccumulation factor estimate (as a median and
338 a 95% uncertainty interval).

339 3.2 GUTS models

340 *3.2.1 Few words about GUTS modelling*

341 All GUTS models are today unified within a theoretical framework describ-
342 ing stressor effects on survival over time, based on hypotheses related to the
343 stressor quantification, the compensatory processes (such as recovery), and
344 the nature of the death process (Jager & Ashauer, 2018). In support of ERA,
345 EFSA considers that both reduced versions of GUTS models (GUTS-RED
346 models) are ready-to-use (Ockleford et al., 2018). To write it simple, these
347 two reduced versions can only be used with standard toxicity test data, that
348 is without measurements of internal damages within organisms. The SD ver-
349 sion (the GUTS-RED-SD model) assumes that all individuals are identically
350 sensitive to the chemical substance by sharing a common internal threshold
351 concentration and that death is a stochastic process once this threshold is ex-
352 ceeded. The GUTS-RED-SD model then describes the instantaneous hazard
353 rate as a threshold function of the damages, themselves described by a very
354 simple TK model. The IT version (the GUTS-RED-IT model) is using the
355 same TK part as the GUTS-RED-SD version. For its TD part, it is based
356 on the critical body residue approach, which assumes that individuals differ in
357 their tolerance threshold when exposed to a chemical compound according to a
358 probability distribution. The GUTS-RED-IT model also assumes that individ-
359 uals die as soon as their internal concentration reaches their individual-specific

360 threshold. By default, the between-individual variability is described by a log-
361 logistic probability distribution.

362 In its recent scientific opinion (Ockleford et al., 2018), EFSA clearly states
363 its support for the use of TKTD models at Tier-2 of ERA according to a
364 specific workflow. Applied in particular for GUTS-RED models, this workflow
365 consists in the following three steps: (1) **Calibration**, which consists in fitting
366 both GUTS-RED models to toxicity test data collected at constant concentra-
367 tion under a standard protocol, in order to get parameter estimates associated
368 with their uncertainty; (2) **Validation**, which consists in simulating the num-
369 ber of survivors over time, using both GUTS-RED models and the previously
370 estimated parameters, but for time-variable exposure profiles under which data
371 have also been collected. The simulated numbers of survivors for both models
372 are then compared to observed ones and the prediction-observation adequacy is
373 checked according to one visual validation criterion together with three quanti-
374 tative validation criteria. These validation criteria were defined by EFSA with
375 the perspective to choose the most appropriate model for the next step; (3)
376 **Prediction**, which consists in simulating the survival probability over time
377 with the previously chosen model and the parameter estimates obtained in step
378 (1), for environmentally realistic exposure scenarios in order to assess risk on
379 how far is the exposure profile from causing a pre-defined effect. Namely, this
380 third step aims at determining the $x\%$ Lethal Profile (denoted LP_x), that is
381 the multiplication factor leading to an additional $x\%$ of reduction in the final

382 survival rate at the end of the exposure. The next subsection guides the reader
383 step by step to perform the EFSA workflow directly using MOSAIC.

384 3.2.2 *MOSAIC_{GUTS-fit}*

385 MOSAIC offers two services related to the use of GUTS-RED models to an-
386alyze standard survival data as function of both time and exposure concen-
387tration: *MOSAIC_{GUTS-fit}* for step (1) and *MOSAIC_{GUTS-predict}* for steps
388(2) and (3). All features of *MOSAIC_{GUTS-fit}* have already been detailed in
389Baudrot et al. (2018b). We just recall here the main highlights: a facilitated up-
390loading of data (either from example data files or from the users themselves),
391an automatic GUTS fitting analysis for either GUTS-RED-SD and GUTS-
392RED-IT models, all useful fitting outputs to check the relevance of the results
393(parameter estimates, fitting curve with its uncertainty, posterior predictive
394check), and a collection of LC_x calculations associated with their uncertainty
395(Figure 4.A). In the following subsection, *MOSAIC_{GUTS-predict}* is presented
396in details, in support of the validation and the prediction steps of the EFSA
397workflow.

398 3.2.3 *MOSAIC_{GUTS-predict}*

399 *MOSAIC_{GUTS-predict}* has been developed in R (R Core Team, 2021) within
400 a Shiny environment (Chang et al., 2021). It is available at <https://mosaic.univ-lyon1.fr/guts-predict> and performed using the computing facilities
401 of the CC LBBE/PRABI. Both steps (2) and (3) of the EFSA workflow require
402

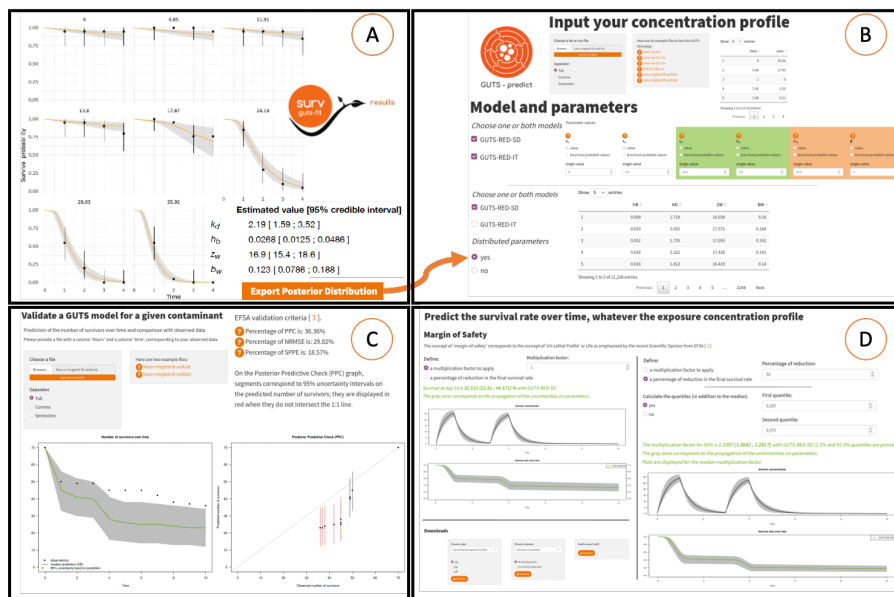


Fig. 4 Selected pieces from MOSAIC for GUTS models: (A) GUTS **calibration** results: model predictions superimposed to the data, parameter estimates and the way to download the joint posterior distribution, from file `Ring-test Dataset B-cst`; (B) GUTS-predict first panel to enter the exposure profile for the simulation (EFSA steps (2) and (3), from file `conc-ringtest-B-varA.txt`), as well as to choose the model to use and how to consider its parameters (distributed or not, from file `mcmc-ringtest-B-SD.txt`); (C) outputs of the EFSA **validation** step (2) where the predicted number of survivors is compared to observed data (from file `Nsurv-ringtest-B-varA.txt`), together with EFSA validation criteria values; (D) outputs of the EFSA **prediction** step (3) where two options are proposed to quantify how far is the exposure profile from causing an $x\%$ effect: fixing the multiplication factor and simulating the predicted survival over time, or fixing x and getting the corresponding multiplication factor; and (E) downloading panel of `MOSAICGUTS-predict`.

403 a time-variable exposure profile that needs to be uploaded first (Figure 4.B).
 404 Then the user can perform simulations with one or both GUTS-RED models,
 405 for which parameter values need to be entered (Figure 4.B). Regarding pa-
 406 rameter values, two options are proposed: only point values (such as means,
 407 medians...) or distributed parameters, namely coming from `MOSAICGUTS-fit`
 408 as the joint posterior distribution, downloadable in advance (Figure 4.A). From
 409 here, users can perform validation step (2) to predict the number of survivors
 410 over time to be compared with observed data ('Validation' tab). For this step,

411 MOSAIC_{GUTS-predict} expects to receive as input both distributed parameters
412 (in order to propagate the uncertainty all along the simulation) and a data
413 file with observations under the uploaded exposure profile (typically a pulsed
414 exposure, Figure 4.C). MOSAIC_{GUTS-predict} returns EFSA validation criteria
415 values together with the simulation superimposed to the observed data and
416 the posterior predictive check (PPC) graph. In the following or independently,
417 the prediction step (3) can be performed to predict the survival probability
418 over time as a function of time under the previously (or a new one) uploaded
419 exposure profile. Usually, for step (3), users are using realistic scenarios, for
420 example predicted environmental concentrations of active substances of plant
421 protection products (European Food Safety Authority, 2017). This prediction
422 step ('Prediction' tab) also requires the use of distributed parameters (namely
423 according to their joint posterior distribution, as delivered in step (1)). From
424 here, users have two options: (i) to fix a multiplication factor (MF) to apply
425 on the uploaded exposure profile and get the prediction as a curve (the median
426 tendency and its uncertainty) associated with the predicted survival probabili-
427 ty at final time; (ii) to fix a percentage of additional reduction on survival at
428 final time (*e.g.*, 20% as on Figure 4.D, left) and ask MOSAIC_{GUTS-predict} to
429 return the corresponding MF that could be applied with a $x\%$ of risk in terms
430 of survival probability for the species-compound combination under interest;
431 this MF is exactly the newly concept of the $x\%$ Lethal Profile (LP_x) as defined
432 by EFSA (Ockleford et al., 2018). Finally, users can download selected pieces
433 of results (Figure 4.D, right).

434 **4 New perspectives for Tier-1 in ERA**

435 As detailed above, TKTD models allow to account for both time and concen-
436 tration in predicting effects due to chemical exposure. In essence, based on
437 standard protocols, TKTD models benefit from all collected data, while dose-
438 response models only rely on data at a fixed target time, that is one of the
439 time points in the experimental design, the most often the end of the experi-
440 ment. Starting from the hypothesis that the gain in knowledge in using TKTD
441 models allow a better precision (or, equivalently, a reduced uncertainty) on pa-
442 rameter estimates, this section highlights the added-value of GUTS models for
443 the estimation of lethal concentration as required for Tier-1 in ERA.

444 As detailed in Baudrot & Charles (2019), the lethal concentration can be
445 obtained from a GUTS model as a continuous function of both the chosen per-
446 centage x and the exposure duration t according to model parameter estimates.
447 Hence, the calculation of any $LC_{(x,t)}$ can be associated to its uncertainty, by
448 propagating the uncertainty associated to model parameter estimates as acces-
449 sible from the joint posterior distribution after performing Bayesian inference.
450 Based on a battery of 20 data sets, the classical LC_{50} value at final time, as esti-
451 mated by a 3-parameters log-logistic model (equation (2)) is compared to the
452 corresponding calculations obtained from both GUTS-RED-SD and GUTS-
453 RED-IT models. The 20 data sets are standard survival data sets with a first
454 set for 10 different species exposed to chlorpyriphos (Rubach et al., 2012),
455 a second for species *Daphnia magna* exposed to seven veterinary antibiotics
456 (Wollenberger et al., 2000) and three other data sets (Forfait-Dubuc et al.,

2012). Each data set was fitted with the three models thanks to the R package
457 **morse** (Baudrot et al., 2021). Note that the entire analysis can be identically
458 reproduced using the MOSAIC platform. For each data set, goodness-of-fit
459 criteria were good enough to support the relevance of the results (see example
460 on Figure 5.A for the data set of *D. magna* exposed to potassium dichromate).
461 So, for each data set, the $LC_{(x,t)}$ estimates (as medians and 95% uncertainty
462 intervals) were collected for $x = 50\%$ and at the end of the experiment, directly
463 from parameter estimates when using the 3-parameters log-logistic model (pa-
464 rameter e in equation (1) above), or asking for the calculation after predicting
465 the dose-response curve with both GUTS-RED models (Figure 5.B).
466

467 Because of different orders of magnitude between LC_{50} estimates among
468 data sets, the three LC_{50} estimates were compared by normalizing them to
469 the classical LC_{50} median estimate obtained with the 3-parameters log-logistic
470 model; this latter having thus a median of 1 (Figure 5.C). Focusing on the only
471 data set of *D. magna* exposed to potassium dichromate (Figure 5.A-C), the
472 starting hypothesis is confirmed with a better precision for both GUTS-RED
473 estimates of the LC_{50} , while both GUTS-RED estimates with a similar preci-
474 sion are not significantly different from the classical calculation (overlapping
475 95% uncertainty intervals). On the basis of this first finding, three questions
476 deserve particular attention: (1) does the better precision depend on the x
477 (first fixed at 50%); (2) does the better precision depend on the exposure
478 duration (first fixed as the experiment duration)? (3) does the better precision
479 depend on the data set, that is on the species? and/or on the compound? As

480 shown on Figure 5.D for the combination *D. Magna*-potassium dichromate,
481 the better precision does not depend neither on x nor on the time at which the
482 $LC_{(x,t)}$ is calculated. Figure 5.D also illustrates that $LC_{(x,t)}$ estimates given
483 by both GUTS-RED models can continuously be obtained whatever t between
484 0 and the exposure duration, but only at time points within the experimental
485 design for the classical estimates with the 3-parameters log-logistic model.

486 Question (3) was answered in two steps. Figure 5.E first shows a slight
487 dependency on the species exposed to chlorpyrifos of the LC_{50} precision,
488 with a similar precision whatever the model for species 03 and 07, while both
489 GUTS-RED estimates are different for species 03, 06 and 08. Secondly, Figure
490 5.F shows a slight dependency again, without high differences between both
491 GUTS-RED estimates, but sometime different from the classic one (compound
492 03 and 09). These results need further investigation for example by looking at
493 the phylogenetic proximity of the 10 compared species as well as at the mode
494 of action of the seven compounds given that our knowledge is still poor in
495 describing how effects vary across both species and compounds (Ashauer &
496 Jager, 2018). Nevertheless, for most of the data set, both GUTS-RED models
497 provide more precise LC_{50} estimates than a classical dose-response approach.
498 Given that all facilities are today available to use GUTS models on standard
499 data sets, the regulatory risk assessment should really consider the possibility
500 to use them even at Tier-1.

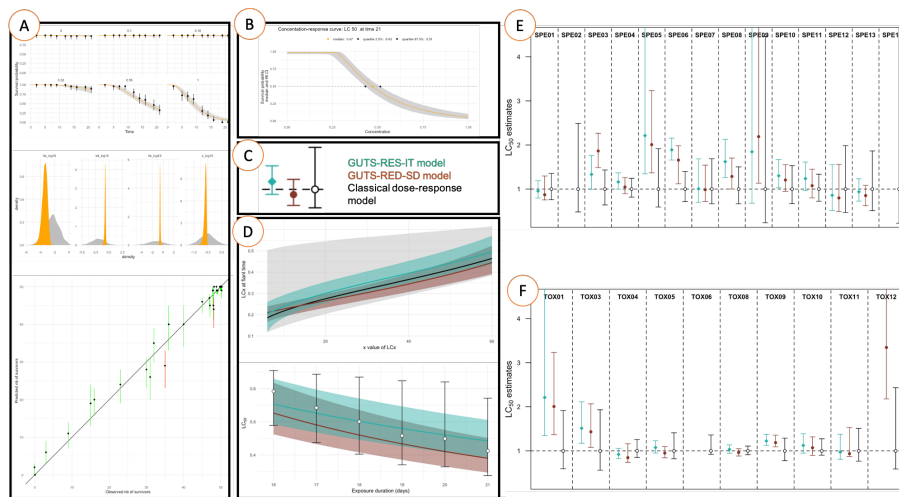


Fig. 5 (A) GUTS-RED-SD fitting results for *Daphnia magna* exposed to potassium dichromate; (B) the corresponding predicted dose-response curve; (C) the three LC_{50} estimates with the 3-parameters log-logistic model (in black), the GUTS-RED-SD model (in red) and the GUTS-RED-IT model (in green); (D) $LC_{x,t}$ calculations for various x (upper panel) and various exposure time (lower panel); (E) comparison of LC_{50} estimates between species exposed to chlorpyrifos; (F) comparison of LC_{50} estimates between compound for *D. magna*.

501 5 Conclusions

502 Although tools are existing to use TKTD models, and although regulatory
503 bodies strongly recommend their use for ERA (especially to facilitate the con-
504 sideration of realistic exposure scenarios), practitioners struggle in appropriate
505 them for reasons mostly attributable to modelers themselves. These reasons
506 mainly come from lack of support: (1) to easily quantify uncertainties, and
507 consequently their propagation to model outputs and subsequent predictions;
508 (2) to better accept changing paradigm using new modelling approaches often
509 appearing as black boxes, together with lack of support to fully perceive the
510 concrete added-value of these novelties for their daily work; (3) to easily inter-
511 pret goodness-of-fit criteria and therefore trust model results in their ability

512 to support decisions from predictions; (4) to appropriate recent user-friendly
513 turn-key facilities, while already recognized as automatically providing toxi-
514 city indices of interest in full compliance with regulatory guidelines and risk
515 assessment decision criteria. The Bayesian inference framework is clearly the
516 direction to take to facilitate the quantification of the uncertainties. In addi-
517 tion, practitioners will be most likely able to accept advanced modelling for
518 ERA if accessibility of modelling is improved in terms of step-by-step support,
519 reproducibility and transparency, founding principles of the web platform MO-
520 SAIC.

521 **6 Ethical Approval**

522 This article does not contain any studies with animals performed by any of
523 the authors.

524 **7 Consent to Participate**

525 All authors participated in the research work underlying the content of the
526 manuscript.

527 **8 Consent to Publish**

528 All authors read and approved the final manuscript for submission.

529 **9 Authors Contributions**

530 SC: coordinated part of the research work underlying the presented results as
531 well as the writing of the manuscript with all contributors; she structured the
532 final version of the manuscript, contributed to figures 2, 4 and 5, and con-
533 ceived the graphical-art figure. AR: drafted the first version of manuscript,
534 conceived figures 1 and 3, reviewed the manuscript and helped in finalizing
535 the submitted version of the manuscript. VB: is the main developer of the
536 **morse** package that supports the MOSAIC web interface; he is actively con-
537 tributing to the MOSAIC_{GUTS-predict}, and reviewed the manuscript. GM: de-
538 veloped the first version of MOSAIC_{bioacc} and made significant improvements
539 in MOSAIC_{growth}, then reviewed the manuscript. AS: is the main developer
540 of MOSAIC_{GUTS-predict}; she reviewed the manuscript and revised figure 4.
541 DW: fully conceived MOSAIC_{growth} in its first version and revised the final
542 manuscript. CL: coordinated part of the research work underlying the pre-
543 sented results and revised the entire manuscript.

544 **10 Funding**

545 The authors are thankful to ANSES for providing the financial support for the
546 development of the MOSAIC_{bioacc} web tool (CNRS contract number 208483).
547 This work was also made with the financial support of the Graduate School
548 H2O'Lyon (ANR-17-EURE-0018) and "Université de Lyon" (UdL), as part

549 of the program “Investissements d’Avenir” run by “Agence Nationale de la
550 Recherche” (ANR).

551 **11 Competing Interests**

552 The authors declare that they have no competing interest.

553 **12 Availability of data**

554 All data used in this paper are downloadable from the MOSAIC web platform.

555 **References**

- 556 Ankley, G., Bennett, R., Erickson, R., Hoff, D., Hornung, M., Johnson, R.,
557 Mount, D., Nichols, J., Russom, C., & Schmieder, P. (2010). Adverse out-
558 come pathways: A conceptual framework to support ecotoxicology research
559 and risk assessment. *Environmental Toxicology and Chemistry*, *29*(3), 730–
560 741.
- 561 Ashauer, R., & Jager, T. (2018). Physiological modes of action across species
562 and toxicants: the key to predictive ecotoxicology. *Environmental Science:
563 Processes and Impacts*, *00*, 1–10.
- 564 Baudrot, V., & Charles, S. (2019). Recommendations to address uncertain-
565 ties in environmental risk assessment using toxicokinetics-toxicodynamics
566 models. *Scientific Reports, Nature Research*, *9*, 11432.

- 567 Baudrot, V., Charles, S., Delignette-Muller, M. L., Duchemin, W., Goussen,
568 B., Kehrein, N., Kon-Kam-King, G., Lopes, C., Ruiz, P., Singer, A., & Veber,
569 P. (2021). *morse: Modelling Tools for Reproduction and Survival Data in*
570 *Ecotoxicology*. R package version 3.3.0.
571 URL <https://CRAN.R-project.org/package=morse>
- 572 Baudrot, V., Preux, S., Ducrot, V., Pave, A., & Charles, S. (2018a). New
573 insights to compare and choose tktd models for survival based on an in-
574 terlaboratory study for *lymnaea stagnalis* exposed to cd. *Environmental*
575 *Science and Technology*, *52*(3), 1582–1590.
- 576 Baudrot, V., Veber, P., Gence, G., & Charles, S. (2018b). Fit Reduced GUTS
577 Models Online: From Theory to Practice. *Integrated Environmental Assess-*
578 *ment and Management*, *14*(5), 625–630.
- 579 Brock, T., Arena, M., Cedergreen, N., Charles, S., Duquesne, S., Ippolito,
580 A., Klein, M., Reed, M., Teodorovic, I., Van den Brink, P. J., & Focks,
581 A. (2020). Application of GUTS models for regulatory aquatic pesticide
582 risk assessment illustrated with an example for the insecticide chlorpyrifos.
583 *Integrated Environmental Assessment and Management*, *00*(00), 1–16.
- 584 Chang, W., Cheng, J., Allaire, J., Sievert, C., Schloerke, B., Xie, Y., Allen,
585 J., McPherson, J., Dipert, A., & Borges, B. (2021). *shiny: Web Application*
586 *Framework for R*. R package version 1.6.0.
587 URL <https://CRAN.R-project.org/package=shiny>
- 588 Charles, S., Veber, P., & Delignette-Muller, M. L. (2018). MOSAIC: a web-
589 interface for statistical analyses in ecotoxicology. *Environmental Science*

- 590 *and Pollution Research*, 25, 11295–11302.
- 591 Charles, S., Wu, D., & Ducrot, V. (2021). How to account for the uncertainty
592 from standard toxicity tests in species sensitivity distributions: An example
593 in non-target plants. *PLOS ONE*, 16(1), e0245071.
- 594 Clements, W. (2000). Integrating effects of contaminants across levels of bio-
595 logical organization: an overview. *Journal of Aquatic Ecosystem Stress and*
596 *Recovery (Formerly Journal of Aquatic Ecosystem Health)*, 7(2), 113–116.
- 597 European Commission (2013). European Commission (EU) No 283/2013 of
598 1 March 2013 setting out the data requirements for active substances, in
599 accordance with Regulation (EC) No 1107/2009 of the European Parliament
600 and of the Council concerning the placing of plant protection product.
- 601 European Food Safety Authority (2017). EFSA Guidance Document for pre-
602 dicting environmental concentrations of active substances of plant protec-
603 tion products and transformation products of these active substances in soil.
604 *EFSA Journal*, 15(178), 1–50.
- 605 Forbes, V. E., & Calow, P. (2002). Species Sensitivity Distributions Revisited:
606 a Critical Appraisal. *Human and Ecological Risk Assessment*, 8(3), 473–492.
- 607 Forbes, V. E., & Galic, N. (2016). Next-generation ecological risk assessment:
608 Predicting risk from molecular initiation to ecosystem service delivery. *En-*
609 *vironment International*, 91, 215–219.
- 610 Forfait-Dubuc, C., Charles, S., Billoir, E., & Delignette-Muller, M. (2012). Sur-
611 vival data analyses in ecotoxicology: critical effect concentrations, methods
612 and models. What should we use? *Ecotoxicology*, 12(4), 1072–1083.

- 613 Grech, A., Brochot, C., Dorne, J.-L., Quignot, N., Bois, F. Y., & Beaudouin,
614 R. (2017). Toxicokinetic models and related tools in environmental risk
615 assessment of chemicals. *Science of the Total Environment*, 578, 1–15.
- 616 Jager, T., & Ashauer, R. (2018). *Modelling survival under chemical stress. A*
617 *comprehensive guide to the GUTS framework*. Leanpub, leanpub ed.
618 URL <https://leanpub.com/guts{ }book>
- 619 Kon Kam King, G., Veber, P., Charles, S., & Delignette-Muller, M. L. (2014).
620 MOSAIC_SSD: a new web tool for species sensitivity distribution to in-
621 clude censored data by maximum likelihood. *Environmental Toxicology and*
622 *Chemistry*, 33(9), 2133–9.
- 623 MOSAIC (2013). Accessed: 2021-03-03.
624 URL <https://mosaic.univ-lyon1.fr/>
- 625 MOSAICbioacc (2020). Accessed: 2021-03-03.
626 URL <https://mosaic.univ-lyon1.fr/bioacc/>
- 627 MOSAICgrowth (2020). Accessed: 2021-03-03.
628 URL <https://mosaic.univ-lyon1.fr/growth/>
- 629 MOSAICguts-fit (2018). Accessed: 2021-03-03.
630 URL <https://mosaic.univ-lyon1.fr/guts/>
- 631 MOSAICguts-predict (2018). Accessed: 2021-03-03.
632 URL <http://lbbe-shiny.univ-lyon1.fr/guts-predict/>
- 633 MOSAICrepro (2014). Accessed: 2021-03-03.
634 URL <https://mosaic.univ-lyon1.fr/repro/>

635 MOSAICssd (2013). Accessed: 2021-03-03.

636 URL <https://mosaic.univ-lyon1.fr/ssd/>

637 MOSAICsurv (2014). Accessed: 2021-03-03.

638 URL <https://mosaic.univ-lyon1.fr/surv/>

639 Ockleford, C., Adriaanse, P., Berny, P., Brock, T., Duquesne, S., Grilli, S.,

640 Hernandez-Jerez, A. F., Bennekou, S. H., Klein, M., Kuhl, T., Laskowski, R.,

641 Machera, K., Pelkonen, O., Pieper, S., Smith, R. H., Stemmer, M., Sundh, I.,

642 Tiktak, A., Topping, C. J., Wolterink, G., Cedergreen, N., Charles, S., Focks,

643 A., Reed, M., Arena, M., Ippolito, A., Byers, H., & Teodorovic, I. (2018).

644 Scientific Opinion on the state of the art of Toxicokinetic/Toxicodynamic

645 (TKTD) effect models for regulatory risk assessment of pesticides for aquatic

646 organisms. *EFSA Journal*, 16(8), 5377.

647 OECD (2012). *Test No. 305: Bioaccumulation in Fish: Aqueous and Dietary*

648 *Exposure*, vol. Section 3. OECD Publishing, Paris.

649 URL <https://doi.org/10.1787/9789264185296-en>.

650 Park, R., Clough, J., & Wellman, M. (2008). AQUATOX: Modeling environ-

651 mental fate and ecological effects in aquatic ecosystems. *Ecological Mod-*

652 *elling*, 213(1), 1–15.

653 Preuss, T., Hommen, U., Alix, A., Ashauer, R., van den Brink, P., Chapman,

654 P., Ducrot, V., Forbes, V., Grimm, V., & Schäfer, D. (2009). Mechanistic

655 effect models for ecological risk assessment of chemicals (MEMoRisk)—a

656 new SETAC-Europe Advisory Group. *Environmental Science and Pollution*

657 *Research*, 16(3), 250–252.

- 658 R Core Team (2021). *R: A Language and Environment for Statistical Com-*
659 *puting*. R Foundation for Statistical Computing, Vienna, Austria.
- 660 URL <https://www.R-project.org/>
- 661 Ratier, A., Lopes, C., Labadie, P., Budzinski, Hélène Delorme, N., Quéau, H.,
662 Peluhet, L., Geffard, O., & Babut, M. (2019). A unified Bayesian frame-
663 work for estimating model parameters for the bioaccumulation of organic
664 chemicals by benthic invertebrates: proof of concept with PCB153 and two
665 freshwater species. *Ecotoxicology and Environmental Safety*, 180, 33–42.
- 666 Ratier, A., Lopes, C., Multari, G., Mazerolles, V., Carpentier, P., & Charles,
667 S. (2020). Brief communication: new perspectives on the calculation of
668 bioaccumulation factors for active substances in living organisms.
- 669 URL <http://dx.doi.org/10.1101/2020.07.07.185835>
- 670 Ritz, C. (2010). Toward a unified approach to dose–response modeling in
671 ecotoxicology. *Environmental Toxicology and Chemistry*, 29(1), 220–229.
- 672 Rubach, M. N., Baird, D. J., Boerwinkel, M.-C., Maund, S. J., Roessink, I., &
673 Van den Brink, P. J. (2012). Species traits as predictors for intrinsic sensi-
674 tivity of aquatic invertebrates to the insecticide chlorpyrifos. *Ecotoxicology*,
675 21(7), 2088–101.
- 676 Schmolke, A., Thorbek, P., Chapman, P., & Grimm, V. (2010). Ecological
677 models and pesticide risk assessment: Current modeling practice. *Environ-*
678 *mental Toxicology and Chemistry*, 29(4), 1006–1012.
- 679 Wollenberger, L., Halling-Sørensen, B., & Kusk, K. O. (2000). Acute and
680 chronic toxicity of veterinary antibiotics to *Daphnia magna*. *Chemosphere*,

681 *40(7)*, 723–730.